Chronology of Pluton Emplacement and Regional Deformation in the Southern Sierra Nevada Batholith, California-Supplementary Data and Discussions

Saleeby, J., Division of Geological and Planetary Sciences, California Institute of Technology, Pasadena, CA 91125
Ducea, M.N., Department of Geosciences, University of Arizona, Tucson, AZ 85721
Busby, C., Department of Geosciences, University of California, Santa Barbara, CA 93106
Nadin, E., Division of Geological and Planetary Sciences, California Institute of Technology, Pasadena, CA 91125
Wetmore, P.H., Department of Geology, University of South Florida, Tampa, FL, 33620

INTRODUCTION

Supplementary data presented here include isotopic and concentration data for U/Pb zircon ages performed by isotope dilution and thermal ionization mass spectrometric (TIMS) techniques (ID-TIMS), for feldspar common lead composition determinations used for nonradiogenic corrections of the zircon data performed by ITMS and U/Pb age data for samples studied by Laser Ablation ICP-MS techniques (Tables DR1, DR2 and DR3, respectively). Supplementary discussions include an overview of the techniques employed for the ID-TIMS technique as well as the single crystal laser ablation ICP multicollector mass spectrometric technique (LA-ICP-MS).

ANALYTICAL TECHNIQUES

Zircon Preparation

Batholithic zircon was separated from 1-5 kg rock samples by standard pulverizing, density contrast, and magnetic susceptibility techniques. Magnetic separation procedures were aimed towards maximum sample purity and selection of highest integrity grains. Non- or paramagnetic zircon was taken from Franz Isodynamic Separator runs with a front slope of 20° and a side slope of either 0° or -1°. After initial washing in 8N, and sieving in expendable nylon sieves, the fractions to be analyzed were picked to 100 percent purity by inspection of each grain. Only well-faceted clear

euhedral grains lacking visible inclusions or cores were accepted. In the early stages of this study some silicic volcanic and hypabyssal samples from the Erskine Canyon sequence that ranged up to 50 kg were used for zircon separations. Separation procedures for these were the same as above, although handpicking was done at a level that could only assure ~99 percent purity, and inspection for grain integrity was not as rigorous. These early samples included E2, E3, E5 and E6.

Select samples for which there was concern for disturbance by superimposed thermal events (E5, D2 and D13) were mechanically abraded to a well rounded state prior to dissolution by techniques similar to Krogh (1982), but with the addition of fine pyrite as an abrading agent. These were given and additional concentrated HNO_3 wash prior to introduction into dissolution capsules. Feldspar separates were split from the separation procedures of samples B2, N4 and D10 for initial lead determinations.

U/Pb Zircon Isotope Dilution Analyses

Zircon separates were weighed into a TFE bomb capsule and then given an additional 15-minute warm wash with ultrapure concentrated HNO_3. Dissolution was performed in concentrated ultrapure HF with a drop of ultrapure concentrated HNO_3 at 225°C for 3 days. Following dissolution, the samples were evaporated and rebombed overnight in ultrapure 6N HC1 prior to spiking. Samples were then spiked with a mixed $^{205}Pb/^{235}U$ tracer, and equilibration was obtained in hot 6N HCL within a sealed PFA container overnight on a hotplate.

Dissolution and chemical extraction techniques for zircon entailed cycles of 2N, 3N and 6N HCl, similar to those described in Krogh (1973). Mass spectrometry was performed on a VG Sector multicollector instrument. Pb and U were run on outgassed Re single filaments with silica gel and graphite loads, respectively. Pb was ionized at ~1400°C and U at ~2000°C, yielding typical ion beam currents of 1 to 5 x 10^{-11} A. Regular inter-calibrations of the multiple detector system yielded stabilities at the 10-ppm level for time periods typically in excess of several hours, and thus Pb and U were run in a static multicollector mode. $^{206}Pb/^{204}Pb$ ratios were measured with the ^{204}Pb beam directed into a Daly deflection knob-photomultiplier system. The gain factor was stable within 5 per mil over the course of the Pb runs. A 0.13±0.05/amu mass fractionation correction was applied to both U and Pb runs based on replicate analyses of NBS 982, 983 and U500 standards. Samples E2, E3, E5 (non-abraded) and E6 were measured during the early stages of this study on the Caltech Lunatic II

single collector thermal ionization mass spectrometer in peak jumping mode. Pb was ionized at ~1150°C yielding a stable ion beam current of 1 to 5 x 10^{-11} A for a period of 2-3 hours, and U at ~1700°C, yielding typical ion beam currents of 1 to 5 x 10^{-11} A stable for periods of ~ 2 hours. A 0.11±0.07/amu mass fractionation correction was applied to U, and 0.12±0.09/amu for Pb runs was applied based on replicate analyses of NBS 982, 983 and U500 standards.

Nonradiogenic lead corrections were based on 25 picogram blank Pb measured at 1:18:78:15:61:38:50 and initial Pb approximations from feldspar determinations (Table DR2). The D1 initial lead values were used for the Erskine Canyon sequence and the Kern River suite samples. The B2 initial lead values were used for Bear Valley suite samples, the N4 values for Needles suite samples, and the D10 values for the Domelands and South Fork suite samples.

Decay constants used in age calculations are $\lambda^{238}U = 1.55125 \times 10^{-10}$ and $\lambda^{235} U = 9.8485 \times 10^{-10}$ (Jaffey and others, 1971). $^{235}U/^{235}U$ atom = 137.88 is after Chen And Wasserburg (1981). Uncertainties in 206Pb*/238U U and $^{206}Pb^*$ are given as ± in last two figures. These uncertainties were calculated by taking the quadratic sum of the total derivatives of ^{238}U and radiogenic ^{206}Pb concentration, and the radiogenic $^{207}Pb/^{206}Pb$ equations with the respective error differentials defined as: 1. Isotopic ratio determinations from standard errors of mass spectrometer runs plus uncertainties in fractionation corrections based on multiple runs of NBS 981, 982, 983 and U500 standards; 2. spike concentrations from range of deviations in multiple calibrations with normal solutions; 3. spike compositions from external precisions of multiple isotope ratio determinations; 4. uncertainty in natural $^{238}U/^{235}U$ from Chen and Wasserburg (1981); and 5. nonradiogenic Pb isotope composition uncertainties in isotope ratio determinations of blank Pb and uncertainties in the isotopic compositions of initial Pb determinations (Table DR2). The error propagation encompasses systematic bias as well as precision factors. Concordia plots presented in Figures 4, 5 and 8 (after Ludwig, 2001) are presented as 2 sigma uncertainties which are nearly identical to the uncertainties shown in Table DR1, and calculated as above.

Feldspar Nonradiogenic Lead Analyses

Powdered feldspar separates were weighed into a TFE bomb capsule and given a warm wash for 15 minutes in ultrapure 4 N HNO_3. Dissolution was complete in concentrated ultrapure HF with 1 drop of ultrapure HNO_3 at

225°C in 24 hours. The solution was evaporated and the feldspar cake was treated with several drops of $HClO_4$ and warmed in the open capsule, evaporated, redissoloved in 6 N HCl and then aliquoted into PFA screw top capsules. One was spiked with a mixed ^{208}Pb-^{235}U-^{230}Th tracer and equilibrated on a hot plate over night. Both aliquots were evaporated, and then redissolved in 6 N HCl-1 N HBr solution. Lead extractions were performed by standard HCl and HBr cycles (cf. Chen and Tilton, 1991), and U-Th extractions were performed for spiked aliquots in HNO_3-HCl cycles. Lead, U and Th were analyzed on VG Sector multicollector thermal ionization mass spectrometer, as above, except Pb was analyzed in a dynamic multicollector peak switching mode while U and Th in static mode.

U/Pb Zircon Laser Ablation Analyses

Select zircon grains from coarse fractions (80-120μ) were mounted in 2.5 cm epoxy mounts and ablated with a New Wave DUV193 Excimer laser, operating with a wavelength of 193 nm and a spot diameter of 35–50 microns. CL images were made for all grains of all mounts and used as a means to screen out grains with clear resorbed or rounded cores or dense inclusion clusters. A sample of typical CL images is given in the included figure. As with most images those shown show pronounced growth zonations whose size nor density apopear to correlate with ages determined. Each grain analysis consists of a single 20-second integration on isotope peaks without laser-firing to obtain on-peak background levels, 20 one-second integrations with the laser firing at the center of each grain, followed finally by a 30-second purge with no laser firing to deliver the remaining evacuated sample. Hg contributions to ^{204}Pb were removed by taking on-peak backgrounds. Each excavation pit is ~20 microns in depth.

The ablated material is carried via argon gas into a Micromass Isoprobe, which is equipped with a flight tube of sufficient width that U and Pb isotopes are measured simultaneously. The measurements are made in static mode, using Faraday detectors for ^{238}U, ^{232}Th, $^{208–206}Pb$, and an ion-counting channel for ^{204}Pb. Ion yields are ~1 millivolt per ppm. Common Pb corrections are made by using the measured ^{204}Pb and assuming initial Pb compositions from Stacey and Kramers (1975). Analyses of zircon grains of known isotopic and U-Pb composition were conducted in most cases after each set of five or ten unknown measurements to correct for elemental isotopic fractionation. In some cases, the standard analyses were sufficiently stable to measure ten unknowns between standards. $^{207}Pb^*/^{206}Pb^*$ ratios for all samples were corrected for 2%–5% ± ~3% fractionation. Common Pb

correction is performed by using the measured ^{204}Pb and assuming an initial Pb composition from Stacey and Kramers (1975) (with uncertainties of 1.0 for $^{206}Pb/^{204}Pb$ and 0.3 for $^{207}Pb/^{204}Pb$). Measurement of ^{204}Pb is unaffected by the presence of ^{204}Hg because backgrounds are measured on peaks (thereby subtracting any background ^{204}Hg and ^{204}Pb), and because very little Hg is present in the argon gas.

For each analysis, the errors in determining $^{206}Pb/^{238}U$ and $^{206}Pb/^{204}Pb$ result in a measurement error of several percent (at 2-sigma level) in the $^{206}Pb/^{238}U$ age. The errors in measurement of $^{206}Pb/^{207}Pb$ are substantially larger for younger grains due to low intensity of the ^{207}Pb signal. The $^{207}Pb/^{235}U$ and $^{206}Pb/^{207}Pb$ ages for younger grains accordingly have large uncertainties, beyond the level of geologic meaning for samples of this study. Inter-element fractionation of Pb/U is generally <20%, whereas isotopic fractionation of Pb is generally <5%. The uncertainty resulting from the calibration correction is generally ~3% (2-sigma) for both $^{207}Pb/^{206}Pb$ and $^{206}Pb/^{238}U$ ages.

The pooled crystallization ages reported in this paper are weighted averages of individual spot analyses. The weighted mean of individual analyses is calculated according to Ludwig (2003). The mean considers only the measurement or random errors (errors in 206Pb/238U and 206Pb/204Pb of each unknown). Age of standard, calibration correction from standard, composition of common Pb, decay constant uncertainty are the other sources that contributed to the error in the final age determination. These uncertainties are grouped and are treated as the systematic error. The error in the age of the sample is calculated by adding quadratically the two components (random or measurement error and systematic error). All age uncertainties are reported at the 2-sigma level (2σ). Only $^{206}Pb/^{238}U$ ages are used in this study because errors of the $^{207}Pb/^{235}U$ and $^{206}Pb/^{207}Pb$ ratios are prohibitive. This is due primarily to the low intensity (commonly <1 mV) of the ^{207}Pb signal from these young, U^{235}-poor grains.

SUPPLEMENTARY REFERENCES

Chen, J.H., and Wasserburg, G.J., 1981, Isotopic determination of uranium in picomole and subpicomole quantities: Anal. Chem., v. 53, p. 2060-2067.

Jaffey, A.H., Flynn, K.F., Glendenin, L.E., Bentley, W.C., and Essling, A.M., 1971, Precision measurement of the half-lives and specific activities of ^{235}U and ^{238}U: Phys. Rev., v. C4, p. 1889-1906.

Krogh, T.E., 1973, A low contamination method for the hydrothermal decomposition of zircon and extraction of U and Pb for isotopic age determinations: Geochem. Cosmochem Acta, v. 37, p. 485-494.

Krogh, T.E., 1982, Improved accuracy of U-Pb zircon ages by the creation of more concordant systems using an air abration technique: Geochem et Cosmochem Acta, v. 46, p. 637-649.

Ludwig, K.R., 2001, Users Manual for Isoplot/Ex (rev. 2.49): A geological toolkit for Microsoft Excel: Berkeley Geochronology Center Spec. Pub. 1a, 56 p.

Stacey, J.S., and Kramers, J.D., 1975, Approximation of terrestrial lead isotopic evolution by a two-stage model: Earth and Planet. Sci Lett., v. 26, p. 207-221.

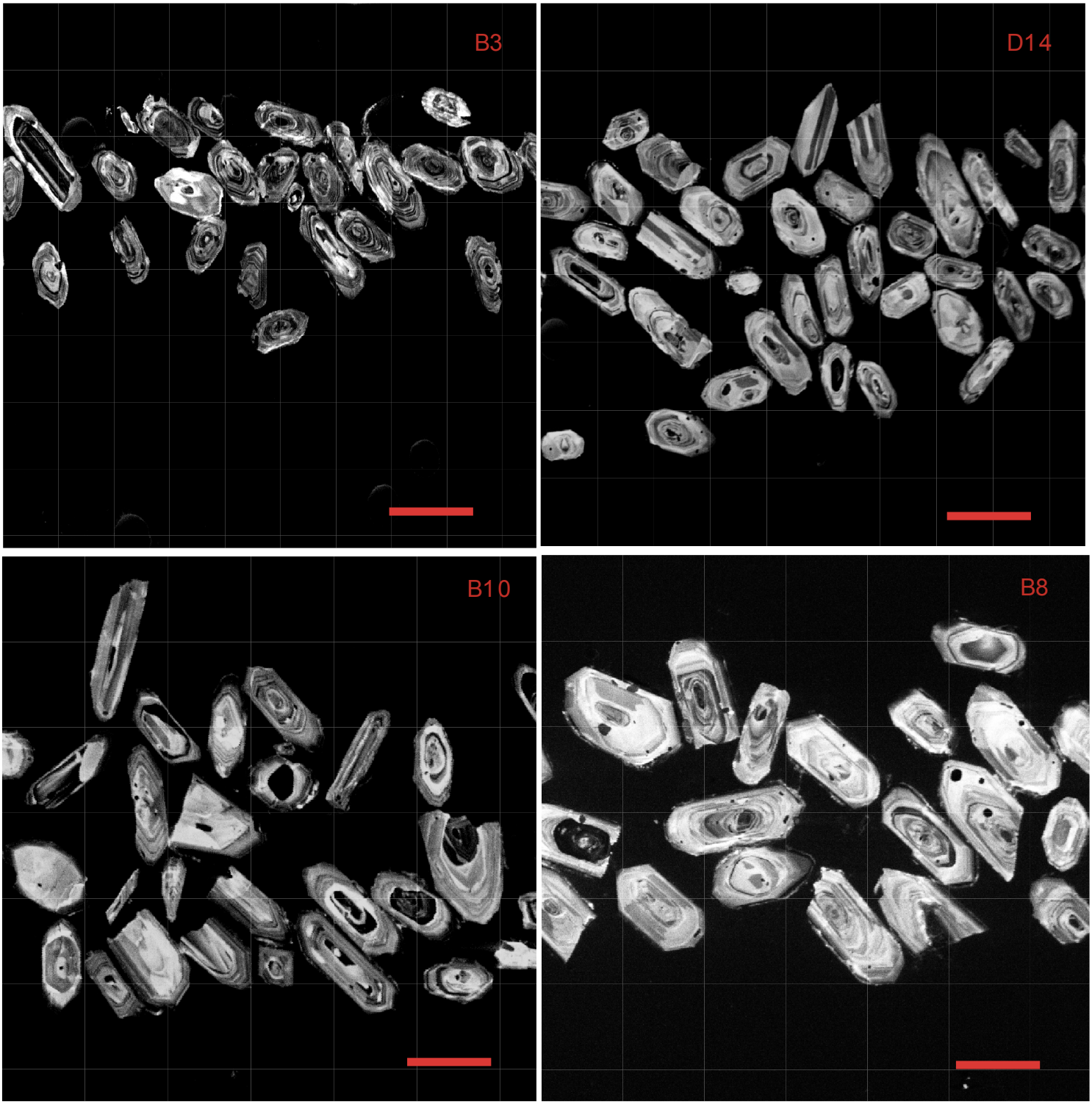

Figure DR1. Backscatted electron SEM photographs using a cathodoluminiscence detector for four representative samples: B3, D14, B10 and B8. The scale bar is 50 microns in lenght for all images.

TABLE DR1: TIMS-ID ZIRCON ISOTOPIC AGE DATA

			Concentrations (ppm)		Atomic ratios*=radiogenic				Isotopic ages (Ma)		
Sample	Fraction (μm) a=abraded	Amount Analyzed (mg)	^{238}U	$^{206}Pb^*$	$^{206}Pb/^{204}Pb$	$^{206}Pb^*/^{238}U$	$^{207}Pb^*/^{235}U$	$^{207}Pb^*/^{235}U$	$^{206}Pb^*/^{238}U$	$^{207}Pb^*/^{235}U$	$^{207}Pb^*/^{206}Pb^*$
Erskine Canyon Sequence											
E1	<45	0.5	724	10.3	2733	0.01637(08)	0.1085	0.04806(05)	104.7	104.6	103
	45-63	0.8	689	9.7	3102	0.01629(08)	0.1082	0.04817(06)	104.2	104.4	108
E2	<45	1.4	1063	15.1	2315	0.01641(14)	0.1093	0.04832(14)	104.9	105.3	115
	45-63	3.3	1045	15.0	971	0.01657(15)	0.1104	0.04839(17)	105.9	106.3	118
	63-80	2.0	837	12.0	893	0.01653(16)	0.1106	0.04851(19)	105.7	106.5	124
E3	<45	3.0	307	4.4	1794	0.01649(15)	0.1099	0.04834(17)	105.5	105.9	116
	45-63	4.1	392	5.6	1513	0.01655(16)	0.1107	0.04853(19)	105.9	106.7	125
	63-80	11.8	453	7.2	1487	0.01661(14)	0.1116	0.04873(19)	106.3	107.5	135
	80-120	8.4	478	7.9	880	0.01899(17)	0.1485	0.05673(23)	121.3	140.5	480
E4	<45	1.2	552	7.8	4231	0.01624(08)	0.1077	0.04810(05)	103.9	103.9	104
	45-63	1.9	461	6.5	2902	0.01628(08)	0.1081	0.04814(06)	104.1	104.2	106
E5	<45	3.9	993	13.3	1921	0.01544(15)	0.1039	0.04882(15)	98.8	100.4	139
	45-63	4.5	814	11.0	2205	0.01562(15)	0.1050	0.04874(14)	99.9	101.4	136
	63-80	7.2	796	10.8	1843	0.01568(15)	0.1075	0.04973(15)	100.3	103.6	135
	<45a	1.1	801	11.2	4739	0.01613(08)	0.1082	0.04864(06)	103.1	104.3	131
	45-63a	2.3	713	10.0	3901	0.01626(08)	0.1104	0.04923(06)	104.0	106.4	159
	63-80a	1.1	629	9.0	3578	0.01654(09)	0.1149	0.05037(07)	105.8	110.5	212
	80-100a	0.6	572	8.4	2983	0.01687(09)	0.1198	0.05149(06)	107.9	114.9	263
E6	<45	1.9	501	7.2	1247	0.01652(15)	0.1116	0.04901(14)	105.7	107.5	148
	45-63	3.4	375	5.6	621	0.01716(16)	0.1222	0.05167(18)	109.7	117.1	271
	63-80	3.1	308	5.0	538	0.01860(16)	0.1442	0.05626(22)	118.8	136.8	462
	80-100	2.4	289	6.3	490	0.02508(24)	0.2517	0.07279(31)	159.7	228.0	1008
Intrusive Suite of the Kern River											
K1	<45	1.1	791	11.2	7920	0.01637(07)	0.1085	0.04809(05)	104.7	104.6	104
	45-63	1.2	613	8.7	6375	0.01647(08)	0.1094	0.04818(05)	105.3	105.5	108
K2	<45	0.9	710	10.0	8593	0.01623(08)	0.1078	0.04816(04)	103.8	104.0	107
	45-63	1.3	667	9.4	7615	0.01634(08)	0.1086	0.04820(05)	104.5	104.7	109
K5	<45	0.9	535	7.5	4992	0.01613(06)	0.1071	0.04815(05)	103.2	103.3	107

Table DR2: Initial lead isotopic data from feldspars.

		Concentrations (ppm)†			Initial ratios*			
Sample	Phase	Pb	U	Th	$\frac{^{206}Pb}{^{204}Pb}$	$\frac{^{207}Pb}{^{204}Pb}$	$\frac{^{208}Pb}{^{204}Pb}$	age (Ma)
K1	k-sp	19.7	1.09	0.96	19.182	15.699	38.989	105
B2	plag	2.1	0.09	0.13	18.849	15.655	38.592	101
N4	k-sp	16.2	0.11	0.19	19.012	15.701	38.901	98
D10	k-sp	20.3	0.59	0.81	18.632	15.601	38.735	89
* 2 sigma uncertainty on initial ratios is ±0.01%.								
†errors in concentration determinations are about ±0.05% for Pb, and ±0.5% for U and Th.								

Table: DR3 continued

sample	U (ppm)	U/Th	6/4c	6/8 ratio	±(%)	6/8 age	±(Ma)	Systematic error
B10								
B10-1	279	1.3	1092	0.01565	2.94	100.1	2.9	1.85
B10-2	78	1.8	292	0.01657	3.14	105.9	3.3	
B10-3	157	1.7	309	0.01548	3.11	99.1	3.1	
B10-4	165	1.5	1028	0.01548	2.17	99.0	2.1	
B10-5	239	1.8	1614	0.01594	2.24	101.9	2.3	
B10-7	284	1.6	1414	0.01541	1.35	98.6	1.3	
B10-8	154	1.8	1101	0.01635	2.46	104.5	2.6	
B10-9	182	1.7	783	0.01599	1.06	102.3	1.1	
B10-10	228	1.6	2039	0.01596	1.44	102.0	1.5	
B10-11	203	1.5	928	0.01562	2.24	99.9	2.2	
B10-12	167	1.8	1170	0.01588	2.85	101.6	2.9	
B10-13	223	1.3	1152	0.01560	3.16	99.8	3.1	
B10-14	220	1.9	1088	0.01549	1.94	99.1	1.9	
B10-15	152	1.8	1229	0.01569	1.18	100.4	1.2	
B10-16	144	1.6	774	0.01601	2.58	102.4	2.6	
B10-17	627	2.5	4265	0.01530	2.79	97.9	2.7	
B10-18	170	1.8	1740	0.01559	1.60	99.7	1.6	
B10-19	204	1.3	2449	0.01564	1.51	100.1	1.5	
B10-20	151	2.2	1502	0.01574	2.36	100.7	2.4	
B10-21	231	1.9	781	0.01553	1.41	99.3	1.4	
B10-22	179	1.9	2148	0.01587	2.23	101.5	2.2	
B10-23	160	2.0	1529	0.01561	1.28	99.9	1.3	
B10-24	184	2.2	1488	0.01558	2.36	99.7	2.3	
B10-25	190	1.7	1944	0.01559	2.29	99.7	2.3	
B10-26	253	1.8	1974	0.01563	1.24	100.0	1.2	
B10-27	194	1.5	992	0.01551	1.74	99.2	1.7	
B10-28	344	1.7	3755	0.01573	1.26	100.6	1.3	
B10-29	227	2.1	2219	0.01565	1.32	100.1	1.3	
B10-30	122	1.9	1067	0.01588	2.49	101.5	2.5	
B10-31	172	2.0	890	0.01569	1.68	100.4	1.7	
B10-32	214	1.3	2563	0.01550	2.28	99.2	2.2	
B10-33	268	2.3	2471	0.01583	1.68	101.2	1.7	
B10-34	155	2.2	1612	0.01568	1.93	100.3	1.9	
B10-35	188	1.4	3218	0.01554	1.02	99.4	1.0	
B10-36	272	1.6	866	0.01552	2.34	99.3	2.3	
B10-37	142	1.6	2969	0.01555	1.54	99.4	1.5	
B10-39	228	1.6	557	0.01539	1.91	98.4	1.9	
B10-40	337	1.5	1266	0.01532	3.75	98.0	3.6	
B10-41	398	1.4	2955	0.01592	2.66	101.8	2.7	
B10-42	240	1.7	1640	0.01551	1.27	99.2	1.2	
B10-43	179	1.6	399	0.01564	1.99	100.1	2.0	
B10-44	191	1.8	909	0.01600	1.81	102.3	1.8	
B10-46	134	1.5	660	0.01561	2.93	99.8	2.9	
B10-47	156	1.6	893	0.01605	2.50	102.7	2.5	
B10-48	244	1.7	1644	0.01541	1.95	98.6	1.9	
B10-49	224	2.5	1294	0.01553	2.11	99.3	2.1	
N10								
N10-1	155	2.5	868	0.05185	12.84	~~325.8~~	~~40.8~~	1.85

Table: DR3 continued

N10-2	96	2.0	523	0.01489	2.40	95.3	2.3	
N10-3	121	1.5	329	0.01409	1.96	90.2	1.8	
N10-4	133	2.2	927	0.01543	3.24	98.7	3.2	
N10-5	191	2.0	396	0.01532	2.12	98.0	2.1	
N10-6	174	1.3	894	0.08708	14.00	~~538.2~~	~~72.3~~	
N10-7	156	1.5	291	0.01510	2.90	96.6	2.8	
N10-9	160	1.5	316	0.01475	3.39	94.4	3.2	
N10-10	129	1.8	542	0.01494	2.72	95.6	2.6	
N10-11	172	1.2	1599	0.01509	2.08	96.6	2.0	
N10-12	120	1.2	414	0.01492	2.62	95.5	2.5	
N10-13	138	1.4	259	0.01498	2.61	95.8	2.5	
N10-14	115	1.8	425	0.01519	3.15	97.2	3.0	
N10-15	123	1.6	272	0.01478	2.08	94.6	1.9	
N10-16	117	1.8	354	0.01532	3.04	98.0	3.0	
N10-17	136	1.3	351	0.01517	4.02	97.1	3.9	
N10-18	168	2.1	736	0.01523	1.67	97.4	1.6	
N10-19	169	1.0	313	0.01447	4.17	92.6	3.8	
N10-20	157	2.1	653	0.01510	3.14	96.6	3.0	
N10-21	85	1.1	417	0.01499	2.69	95.9	2.6	
N10-25	197	3.5	2935	0.01521	3.65	97.3	3.5	
N10-26	81	1.8	1127	0.01542	3.42	98.6	3.3	
N10-27	84	2.0	375	0.01525	3.14	97.6	3.0	
D1								
D1-1	141	1.1	797	0.01430	2.11	91.5	1.9	1.85
D1-2	144	1.5	453	0.01473	2.01	94.3	1.9	
D1-3	175	1.7	370	0.01514	5.80	96.9	5.6	
D1-4	801	3.1	1890	0.01534	1.24	98.1	1.2	
D1-5	207	0.9	300	0.01499	3.00	95.9	2.9	
D1-6	158	1.0	323	0.01552	3.99	99.3	3.9	
D1-7	56	1.5	210	0.01521	7.78	97.3	7.5	
D1-8	125	1.5	638	0.01465	2.12	93.7	2.0	
D1-9	457	1.0	494	0.01491	3.76	95.4	3.6	
D1-11	319	1.9	1425	0.01497	3.28	95.8	3.1	
D1-12	82	1.4	415	0.01468	3.68	93.9	3.4	
D1-14	214	1.7	1144	0.01411	1.22	90.3	1.1	
D1-15	660	2.7	1625	0.01493	1.96	95.5	1.9	
D1-16	393	1.9	2038	0.01459	1.14	93.4	1.1	
D1-17	169	1.3	585	0.01505	3.44	96.3	3.3	
D1-18	600	4.2	733	0.01502	1.90	96.1	1.8	
D1-20	142	1.5	1422	0.01487	3.75	95.2	3.5	
D1-21	453	1.5	880	0.01454	1.82	93.0	1.7	
D1-22	371	7.4	1031	0.01508	1.03	96.5	1.0	
D1-24	137	1.1	293	0.01471	4.30	94.2	4.0	
D1-25	297	1.4	429	0.01467	2.61	93.9	2.4	
D1-26	152	1.4	445	0.01481	2.16	94.8	2.0	
D3								
~~D3-3~~	~~140~~	~~4.5~~	~~1379~~	~~0.02540~~	~~11.26~~	~~161.7~~	~~18.0~~	3.6
D3-5	211	2.4	994	0.01470	2.39	94.1	2.2	
D3-7	39	1.0	285	0.01483	9.59	94.9	9.0	
D3-10	112	1.5	528	0.01516	4.23	97.0	4.1	
D3-11	227	1.0	913	0.01476	3.59	94.5	3.4	

Table: DR3 continued

D3-12	41	1.1	378	0.01393	6.02	89.2	5.3	
D3-13	137	1.1	1015	0.01419	3.60	90.8	3.3	
D3-14	146	1.1	763	0.01455	3.15	93.1	2.9	
D3-15	298	1.1	3247	0.01425	2.09	91.2	1.9	
D3-16	83	1.1	279	0.01717	6.19	109.7	6.7	
D3-20	90	1.7	197	0.01418	11.31	90.8	10.2	
D3-21	266	1.5	724	0.01464	13.92	93.7	12.9	
D3-23	319	2.4	1155	0.01520	4.62	97.3	4.5	
~~D3-24~~	~~32~~	~~2.8~~	~~592~~	~~0.03635~~	~~15.90~~	~~230.2~~	~~36.0~~	
D3-28	289	1.0	671	0.01499	7.39	95.9	7.0	
D3-29	170	1.5	260	0.01615	7.99	103.3	8.2	
D3-30	540	3.7	2031	0.01381	6.10	88.4	5.4	
D3-31	478	0.2	1060	0.01520	3.01	97.2	2.9	
~~D3-32~~	~~217~~	~~1.2~~	~~840~~	~~0.01870~~	~~4.69~~	~~119.4~~	~~5.5~~	
D3-33	282	1.2	226	0.01409	7.25	90.2	6.5	
D3-34	102	1.1	220	0.01423	7.67	91.1	6.9	
D3-38	310	1.4	697	0.01420	5.66	90.9	5.1	
D3-42	188	2.9	311	0.01387	8.04	88.8	7.1	
D3-43	382	3.9	788	0.01410	2.98	90.3	2.7	
D3-44	312	1.2	319	0.01641	3.70	104.9	3.8	
D3-45	107	1.1	166	0.01500	10.53	96.0	10.0	
D3-46	557	1.4	1802	0.01413	3.16	90.4	2.8	
D3-47	227	2.4	375	0.01712	5.83	109.4	6.3	
D3-48	259	1.2	500	0.01561	4.23	99.8	4.2	
D3-49	297	2.4	903	0.01421	5.02	91.0	4.5	
D3-50	360	1.3	1210	0.01506	5.32	96.4	5.1	
D9								
D9-1	599	0.9	3658	0.01424	1.01	91.1	0.9	3.4
D9-2	524	1.1	1502	0.01381	1.22	88.4	1.1	
D9-3	472	1.1	814	0.01387	1.10	88.8	1.0	
D9-4	617	0.7	1480	0.01423	1.07	91.1	1.0	
D9-5	201	1.1	472	0.01387	1.37	88.8	1.2	
D9-7	690	1.0	1852	0.01409	1.71	90.2	1.5	
D9-6	555	0.7	1385	0.01395	1.08	89.3	1.0	
D9-8	521	1.0	960	0.01412	1.82	90.4	1.6	
D9-9	398	1.0	1805	0.01372	1.16	87.8	1.0	
D9-10	591	1.1	1571	0.01405	1.23	90.0	1.1	
D9-11	306	1.3	1460	0.01401	1.23	89.7	1.1	
D9-12	637	0.6	1154	0.01372	1.51	87.9	1.3	
D9-13	403	0.7	241	0.01417	1.82	90.7	1.6	
D9-14	622	0.9	1042	0.01412	1.43	90.4	1.3	
D9-15	600	0.9	577	0.01358	1.85	87.0	1.6	
D9-16	528	0.8	951	0.01413	1.46	90.4	1.3	
D9-17	204	1.2	720	0.01419	2.70	90.8	2.4	
D9-18	313	1.1	1836	0.01386	1.35	88.8	1.2	
D9-19	319	1.6	4442	0.01429	2.29	91.5	2.1	
D9-20	457	0.8	2175	0.01378	2.97	88.3	2.6	
D9-21	338	0.7	443	0.01408	1.58	90.1	1.4	
D9-22	348	0.9	428	0.01380	1.44	88.3	1.3	
D9-24	295	0.9	1999	0.01356	2.25	86.8	1.9	
D9-25	349	1.4	2643	0.01414	2.62	90.5	2.4	
D9-26	350	1.4	3058	0.01413	1.73	90.5	1.6	

Table: DR3 continued

S2								
S2-1	247	1.0	1828	0.01532	1.45	98.0	1.4	1.97
S2-5	198	0.9	843	0.01577	3.57	100.8	3.6	
S2-6	217	1.1	4627	0.01538	1.92	98.4	1.9	
S2-7	321	1.1	4246	0.01522	2.03	97.4	2.0	
S2-8	207	1.0	4756	0.01546	2.18	98.9	2.1	
S2-9	325	0.8	4402	0.01510	1.47	96.6	1.4	
S2-10	315	0.8	2573	0.01544	2.32	98.8	2.3	
S2-11	182	1.0	1142	0.01566	3.12	100.1	3.1	
S2-12	297	0.8	1895	0.01569	2.50	100.3	2.5	
S2-13	201	0.9	2648	0.01549	1.82	99.1	1.8	
S2-14	307	0.9	11944	0.01556	1.08	99.5	1.1	
S2-15	235	1.9	2491	0.01520	1.19	97.2	1.2	
S2-16	244	1.1	5660	0.01551	2.17	99.2	2.1	
S2-17	110	1.3	1426	0.01559	3.12	99.7	3.1	
S2-18	199	1.9	2693	0.01558	1.98	99.6	2.0	
S2-19	259	0.8	5493	0.01578	1.60	100.9	1.6	
S2-20	316	0.8	5382	0.01532	1.80	98.0	1.8	
S2-21	303	0.8	2604	0.01581	1.92	101.1	1.9	
S2-22	271	1.0	3391	0.01602	1.44	102.5	1.5	
S2-23	193	1.1	1850	0.01565	1.20	100.1	1.2	
S2-24	213	0.9	3786	0.01579	2.53	101.0	2.5	
S2-25	282	0.8	2908	0.01616	2.39	103.3	2.5	
S2-26	383	0.7	5970	0.01555	1.23	99.5	1.2	
S2-28	230	0.7	2414	0.01581	2.64	101.1	2.6	
S6								
S6-1	160	2.2	1717	0.01519	4.05	97.2	3.9	1.97
S6-2	147	1.9	1377	0.01525	1.77	97.6	1.7	
S6-3	175	1.4	2127	0.01478	1.53	94.6	1.4	
S6-4	150	1.3	1084	0.01520	2.16	97.3	2.1	
S6-5	161	1.2	1264	0.01537	2.93	98.3	2.9	
S6-6	130	1.4	970	0.01467	2.48	93.9	2.3	
S6-7	199	1.7	2775	0.01464	2.04	93.7	1.9	
S6-8	192	1.0	1988	0.01488	1.56	95.2	1.5	
S6-9	200	1.2	2457	0.01491	2.43	95.4	2.3	
S6-10	91	0.9	534	0.01522	5.21	97.4	5.0	
S6-11	191	1.3	2153	0.01453	1.72	93.0	1.6	
S6-12	144	1.2	1824	0.01475	2.25	94.4	2.1	
S6-13	151	1.2	567	0.01478	1.69	94.6	1.6	
S6-14	212	1.0	1264	0.01453	2.19	93.0	2.0	
S6-15	195	1.3	1937	0.01476	2.16	94.4	2.0	
S6-16	156	1.1	1547	0.01476	2.31	94.5	2.2	
S6-17	131	1.2	499	0.01492	2.17	95.5	2.1	
S6-18	139	1.8	483	0.01472	2.28	94.2	2.1	
S6-19	218	1.6	2214	0.01481	1.65	94.8	1.6	
S6-20	193	1.4	754	0.01431	2.27	91.6	2.1	
S6-21	206	1.0	1292	0.01554	2.56	99.4	2.5	
S6-22	189	0.9	2281	0.01510	1.97	96.6	1.9	
S6-23	127	1.1	553	0.01482	4.79	94.9	4.5	
S6-24	214	1.4	2692	0.01457	2.04	93.2	1.9	

Table: DR3 continued

B8								
B8-1	367	1.7	893	0.01522	1.41	97.4	1.4	3.6
B8-2	372	1.7	936	0.01581	1.64	101.1	1.6	
B8-3	456	1.9	644	0.01560	2.55	99.8	2.5	
B8-4	354	1.8	835	0.01504	1.27	96.2	1.2	
B8-5	292	1.8	792	0.01495	2.00	95.6	1.9	
B8-6	361	2.6	601	0.01579	2.10	101.0	2.1	
B8-7	303	2.0	680	0.01517	2.16	97.1	2.1	
B8-8	448	2.6	689	0.01575	1.53	100.8	1.5	
B8-9	330	1.4	576	0.01541	1.02	98.6	1.0	
B8-10	335	1.8	982	0.01532	2.02	98.0	2.0	
B8-11	510	1.8	1657	0.01528	1.01	97.8	1.0	
B8-12	363	1.7	1306	0.01515	2.61	96.9	2.5	
B8-13	790	1.5	905	0.01523	3.61	97.4	3.5	
B8-14	375	2.2	697	0.01552	2.59	99.3	2.5	
B8-15	341	1.9	1608	0.01516	1.26	97.0	1.2	
B8-16	656	1.5	1304	0.01511	2.53	96.7	2.4	
B8-17	451	1.5	529	0.01516	1.12	97.0	1.1	
B8-18	263	1.7	1273	0.01525	1.43	97.6	1.4	
B8-19	240	2.1	996	0.01511	2.13	96.7	2.0	
B8-20	170	1.6	239	0.01568	2.67	100.3	2.7	
B8-21	497	1.5	1552	0.01542	2.13	98.7	2.1	
B8-22	263	4.0	1781	0.01539	1.14	98.5	1.1	
B8-23	270	1.5	1265	0.01518	2.71	97.1	2.6	
B8-24	399	1.5	1641	0.01517	1.03	97.0	1.0	
B8-25	221	1.8	1074	0.01572	1.35	100.5	1.4	
B8-26	416	1.6	875	0.01512	1.71	96.7	1.6	
B8-27	240	2.3	1308	0.01562	1.54	99.9	1.5	
B8-28	352	1.9	2121	0.01515	1.69	96.9	1.6	
B8-29	271	2.0	1419	0.01546	1.26	98.9	1.2	
B8-30	190	1.9	816	0.01548	2.89	99.0	2.8	
B8-31	264	2.1	1199	0.01580	2.08	101.0	2.1	
B8-32	230	1.7	804	0.01558	1.33	99.7	1.3	
B8-34	236	2.4	1156	0.01551	1.80	99.2	1.8	
B8-35	246	2.7	1126	0.01560	1.52	99.8	1.5	
B8-36	260	1.7	1237	0.01548	2.04	99.0	2.0	
B8-37	324	1.8	1869	0.01565	1.43	100.1	1.4	
B8-38	373	1.4	1134	0.01513	1.02	96.8	1.0	
B8-39	207	1.8	993	0.01537	1.56	98.3	1.5	
B8-40	301	1.9	763	0.01563	1.88	100.0	1.9	
B8-41	251	1.8	1340	0.01577	1.58	100.9	1.6	
B8-42	447	2.3	1846	0.01564	1.01	100.1	1.0	
B8-43	273	2.0	440	0.01517	1.50	97.0	1.4	
B8-44	263	1.7	1994	0.01505	1.49	96.3	1.4	
B8-46	315	1.8	1172	0.01526	1.28	97.7	1.2	
B8-47	344	2.0	1376	0.01539	1.01	98.5	1.0	
B8-48	401	2.0	1183	0.01507	2.79	96.4	2.7	
B8-50	387	1.4	1437	0.01509	1.09	96.5	1.0	